Chapter 12
Electrocavitation in Nanochannels

Daniel S. van Schoot, Kjeld G.H. Janssen, Niels R. Tas, Thomas Hankemeier, and Jan C.T. Eijkel

Abstract A novel method has been developed to cavitate aqueous solutions, which is called electrocavitation. An axial voltage is applied in a nanochannel containing an aqueous solution with a stepwise conductivity gradient. A combination of electrical and viscous forces then generates a tension in the solution which, at sufficiently low pressures, causes it to cavitate. Measurement of the current during the experiment as well as optical observation provides knowledge on the time and axial position of cavitation, after which the pressure at the cavitation position can be calculated from a theoretical model in which also the ζ-potential is inserted, which is separately determined from electroosmotic flow experiments. It is found that generally the cavitation position coincides with the position of the conductivity step. In several experiments the cavitation pressure in successive experiments on the same channel became increasingly lower, suggesting a gradual removal of cavitation nuclei from the system. We calculated that pressures as low as -1630 bar ± 10 % have been reached, close to theoretically predicted pressures for homogeneous cavitation. The platform performs reliably and can be easily controlled.

D.S. van Schoot • J.C.T. Eijkel
BIOS-Lab on a Chip Group, Mesa+ Institute for Nanotechnology, University of Twente, Enschede, The Netherlands
e-mail: j.c.t.eijkel@utwente.nl

K.G.H. Janssen • T. Hankemeier
Department of Analytical Biosciences, Leiden/Amsterdam Centre for Drug Research (LACDR), Leiden University, Leiden, The Netherlands

N.R. Tas (✉)
Department of Transducers Science and Technology, MESA+ Institute for Nanotechnology, University of Twente, Enschede, The Netherlands
e-mail: n.r.tas@utwente.nl

12.1 Introduction

The cavitation of water is a subject of considerable interest for water transport in confined spaces such as in soil and trees and thus is studied both theoretically and experimentally [1]. Water drainage from soil for example can be facilitated by cavitation events [2]. Thermodynamics predicts pure water to become unstable and cavitate at the spinodal pressure, which at 300 K is estimated to lie between $-1,500$ and $-2,000$ bar [1, 3]. Experimentally, the spinodal pressure cannot be reached since cavitation occurs at lower pressures. In general during experiments both heterogeneous and homogeneous cavitation can occur. Homogeneous cavitation occurs in the water itself by loss of cohesion between its molecules, and thus can provide information on the spinodal pressure. The homogeneous cavitation pressure expected in a certain experiment can be calculated by assuming that cavitation nuclei are continuously generated by thermal movement and that after nucleation surface tension strives to close the nucleus while the pressure difference between nucleus and water strives to expand it. Cavitation then occurs when the latter prevails. In such calculations the homogeneous cavitation pressure of pure water depends on temperature, observation time and volume and at 300 K lies between $-1,400$ and $-1,900$ bar [4]. Heterogeneous cavitation on the other hand occurs at the interface of water and surfaces such as container walls, or at the interface of water and impurities such as particles or dissolved molecules. When it occurs it makes it impossible to obtain the homogeneous cavitation pressure. The properties of the surface or the impurity are here of central importance. Most often pre-existing bubbles are thought to act as nucleation sites, which can for example be stabilized in surface cracks or by layers of adsorbed substances [1].

In cavitation studies metastable water is created either by superheating or by stretching [1]. Mainly three experimental platforms exist for the study of cavitation by stretching: centrifugation of a tube filled with liquid perpendicular to its axis [5], an acoustic wave generated by a piezo-electric transducer [3] and heating of water inclusions in quartz inclusions followed by cooling until cavitation occurs [6]. The former two methods quite reproducibly yield cavitation pressures around -260 bar at 0 °C, while the latter method shows much less reproducibility but has yielded cavitation pressures down to $-1,400$ bar at 40 °C, close to the theoretical estimates [5]. To explain the discrepancy between the different methods, ubiquitous stabilizing impurities have been assumed for the quartz inclusion experiments (such as hydroxyl ions) or ubiquitous destabilizing impurities for the other methods (such as hydronium ions) [7]. Shmulovich et al. explicitly studied the (de)stabilizing influence of different electrolytes on the cavitation pressure of water in quartz inclusions [8].

Recently we introduced a new platform to generate negative pressures which we called electrocavitation [9]. The method relies on the generation of strong electrical and restoring shear forces in an aqueous electrolyte solution filling a nanometer-scale channel. Since our experimental procedure relies on the presence of dissolved ions, no data on pure water can be obtained. The procedure however

is eminently useful to investigate cavitation of aqueous salt solutions and especially the influence of different salts. Since the procedure furthermore is rapid, a sequence of experiments can be performed on the same channel yielding additional valuable information.

12.2   Experimental Section

Channels of nanometer scale depth ('nanochannels') were manufactured in the cleanroom of the University of Twente in borofloat glass wafers using lithography and wet HF etching. The height of the channels was determined using a mechanical surface profiler (Dektak 8, Veeco Instruments Inc. Plainview, USA) and found to be uniform over the entire wafer at approximately 53 nm. The channel wafer was thermally bonded to a second wafer and annealed. Subsequently through holes were supersonically drilled. Each wafer contained 19 single channels, six 20 μm wide, seven 10 μm wide and six 5 μm wide. The channel length was 35 mm and all channels had rulers and a unique identifier. In this study only the 10 μm wide channels were utilised.

A custom-built chip interface provided tubing inlets from the top and below, aligned with the nanochannel access holes (Fig. 12.1). The table with the interface
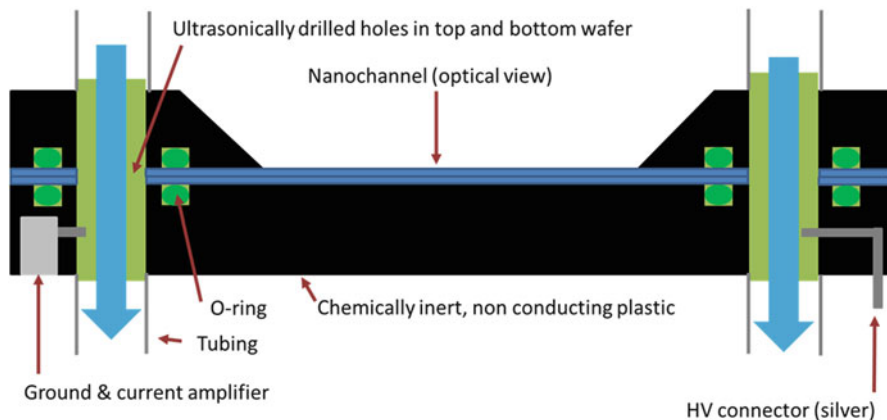

Fig. 12.1 Cross section of the interface holding the wafer. The wafer can be aligned such that one nanochannel can be selected, as is the case in the picture. The drilled holes were then aligned with the tubing through which liquid can be pumped in the direction indicated by the *blue arrows*. The liquid can make its way into the nanochannel by either capillary filling or by applying a voltage between the High Voltage (*HV*) connector (*on the right*) and ground (*on the left*), creating electroosmotic flow (*EOF*). These two connectors were connected to the power source by a coax-cable. The nanochannels can be optically viewed from above as indicated by the *arrow*. Elastic O-rings were manually placed into the setup to prevent any leakage. Silver/silver chloride electrodes were employed for voltage application and current measurement

Table 12.1 The solutions used in the cavitation experiments

Salt used	Concentration (mM)	Ionic strength (mM)	Approximate conductivity (mS/cm)
NaHEPES	5	5	0.39
NaCl	9	9	1.35
	10	10	1.35

can be moved to optically determine the exact position of cavitation. The liquids were pumped through the wafer through-holes by a syringe pump (Harvard Apparatus, USA). Voltages between -3 and $+3$ kV were applied using a HSV488 6000D power supply (LabSmith inc., Livermore, USA) controlled by a LabView script. This same script was used to start and stop measurements. Data was gathered at the ground electrode, which is connected to a current-to-voltage (IV) converter and then to a DAC-PCI card at the PC. This IV converter converts the current into a voltage and amplifies it by a factor 10^8 for the PCI-card. A specific voltage source provides the IV converter circuit with the necessary voltages ($+2.5$ and -2.5 V). The PCI-card has an input range of about -2.2 to $+2.2$ V, which translates to a current between -22 and $+22$ nA. Digital (pre)processing and analysis of the data was performed using Matlab (MathWorks Inc., Natick, USA). The syringes, tubing and waste containers were extensively shielded and connected to ground. An Olympus BX51WI microscope was used for optical inspection with bright field and fluorescence imaging, equipped with a long pass filter cube (488 nm excitation, 518 nm emission), using a 10X magnification objective with a numerical aperture of 0.25 (Olympus Corporation, Tokyo, Japan). Images and movies were recorded using a Hamamatsu Orca-ER CCD camera and included HOKAWO software (HAMAMATSU Photonics K.K., Japan) for reference and checking purposes.

The solutions used are shown in Table 12.1. We chose both salts to have sodium (Na^+) as the cation, so that a single counterion is present in the electrical double layer along the channel axis and the axial uniformity of the ζ-potential during the experiment is increased. The ζ-potential will generally be <-25 mV and therefore will be proportional to the square root of the ionic strength which is also given in Table 12.1.

The proper functioning of the current measurements was checked with high resistance, high voltage resistors (Hymeg Corporation, Addison, USA). To determine the ζ-potential, the electroosmotic flow (EOF) velocity was determined for every channel prior to cavitation experiments, using the same salt solutions. By applying a relatively low voltage (under 500 V), a low conductivity solution was replaced by a high conductivity solution. From the time needed for the current to increase to a new plateau value the EOF velocity can then be derived, which yields the ζ-potential [10].

A schematic overview of a typical measurement cycle is shown in Fig. 12.2. After the initial filling of the channel from the high voltage side by capillary action (2A and B), both through holes were flushed with their respective solutions. After this initial filling or a cavitation experiment the channel was filled entirely by EOF with

Fig. 12.2 Experimental procedure for one cycle of the electrocavitation experiments (see text)
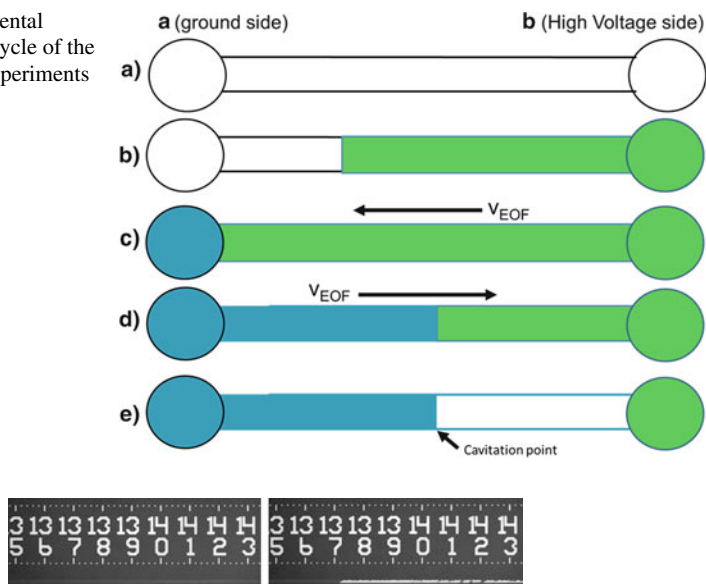

Fig. 12.3 A cavitation event. In this case the low conductivity fluid is drained to the right. The difference between the two pictures is one frame of 0.2 s. The cavitation front stays in place at 13.72 mm. This position can be compared to the position of the interface between the two solutions of different conductivity which can be theoretically predicted from the ζ potential and applied voltage

low conductivity solution by applying 500 V over the channel for 60 or 90 s (2C). The voltage was then lowered to 0 V for 20 s and liquid was pumped through the through holes. The voltage was subsequently reversed to $-1{,}000$ V, $-2{,}000$ V or $-3{,}000$ V for 60 s. The high conductivity solution will now move into the channel by EOF (2D), causing the pressure to decrease and leading to cavitation (2E). Cavitation was detected both optically and electrically. The cavitation time was taken directly from the current measurements since a substantial current decrease was observed. The position was also determined optically as usually one of the solution fronts remained in place. The voltage was then turned off again for 20 s and the channel started to refill by capillary action while fresh fluid was pumped through the through holes. The cycle from C to E was then repeated by setting the voltage to 500 V again for 60 or 90 s. Each experiment consisted of four cycles.

12.3 Experimental Results and Discussion

In each channel, after determining the ζ-potential, electrocavitation experiments were performed. Two subsequent recorded frames of a cavitation event are shown in Fig. 12.3.
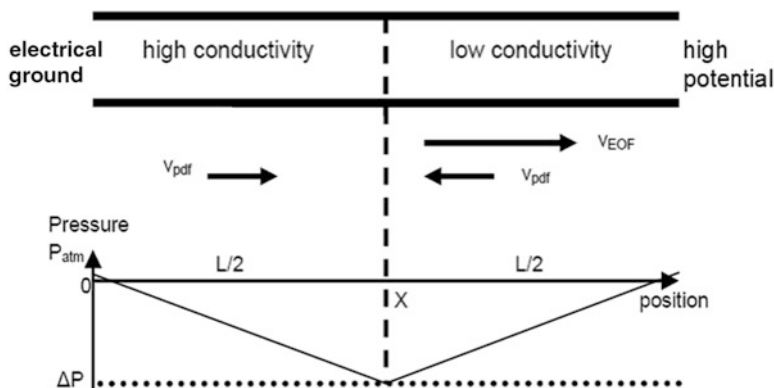
Fig. 12.4 Schematic drawing of a nanochannel containing two adjacent electrolyte solutions, each occupying half of the channel. The difference in conductivity between both solutions is assumed to be very large, limiting the axial electrical field to the low-conductivity half where it generates EOF. To assure a constant axial volume flow (as imposed by mass conservation), a pressure gradient is generated as indicated, generating flow against the EOF at the right-hand side and with the EOF at the left-hand side (*arrows*), and creating a negative pressure in the channel

The cavitation generation mechanism is thought to be the following. When a nanochannel is filled with adjacent solutions of high and low conductivity (Fig. 12.4), an applied axial potential difference will drop predominantly over the low-conductivity solution, inducing a locally stronger EOF. To satisfy a continuous mass flow a pressure gradient arises, generating liquid flow against the EOF in the low-conductivity part and with the EOF in the high conductivity part. Due to the high hydrodynamic resistance of a nanochannel this pressure gradient is very large, resulting in a very low pressure at the interface between the two solutions.

An order of magnitude estimate of the generated negative pressure is obtained by assuming that each electrolyte fills half of the nanochannel and that the potential drop over the high-conductivity part can be neglected. It then follows from the equations of pressure-driven flow and EOF [11] that the generated pressure drop, ΔP, from the reservoirs to the midpoint in the channel is

$$\Delta P = -\frac{6\epsilon\zeta V}{h^2}$$

where ε (F/m) is the dielectric constant of the solution, ζ (V) the zeta potential, V (V) the applied potential difference and h (m) the channel height. For $\varepsilon = 7.5 \cdot 10^{-10}$ F/m, $\zeta = -50$ mV, h $= 50$ nm and V $= -3,000$ V a negative pressure of $-2,750$ bar results. This very low value indicates the potential of this method for liquid cavitation studies. Using a similar but more elaborate theory, we theoretically predicted the time dependent pressure profile in the channel in the remainder of this chapter.

A representative example of an electrocavitation current measurement at 1 kV is shown in Fig. 12.5, and shows one of the four cycles of which an experiment
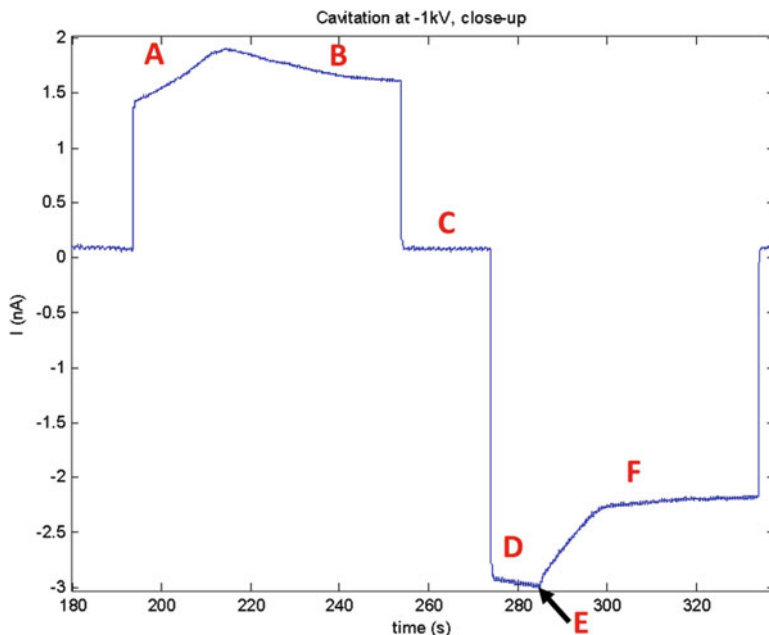
Fig. 12.5 One cycle of an electrocavitation measurement at −1 kV. See the text for the annotated characters A–F

consists. The applied voltage is positive at first, so the NaHEPES solution will start refilling the emptied (from a previous cavitation event) channel both by capillary forces and EOF. This causes the current to rise as the conductivity greatly increases from very low (i.e. empty channel) to that of the NaHEPES solution (A and Fig. 12.2A and B). At some point, depending on where the cavitation in the previous experiment took place, the channel will be fully filled with solution again. Now the EOF starts to displace the NaCl solution with NaHEPES solution. This lowers the current since NaHEPES has a lower conductivity than NaCl. (B) As the whole channel gets filled with NaHEPES, the current stabilises. The voltage is then turned off to pump and refresh the two solutions through the holes (C). Next, −1 kV is applied over the channel. The channel starts filling with NaCl solution again, making the current rise (D and Fig. 12.2D). At some point the pressure can become so low that the solution cavitates (E and Fig. 12.2E). The channel drains and a residual electrical current remains, most likely due to surface conduction (F). The voltage is then turned off and the channel fills by capillary action while new solution is pumped through the holes. The cycle then starts again.

The cavitation position is noted as the location where the liquid meniscus is located after cavitation. Numerous optical observations confirmed that this is the same place as where cavitation takes place, within a distance of maximally 50 μm, which defines the error on the cavitation position. The cavitation time from the
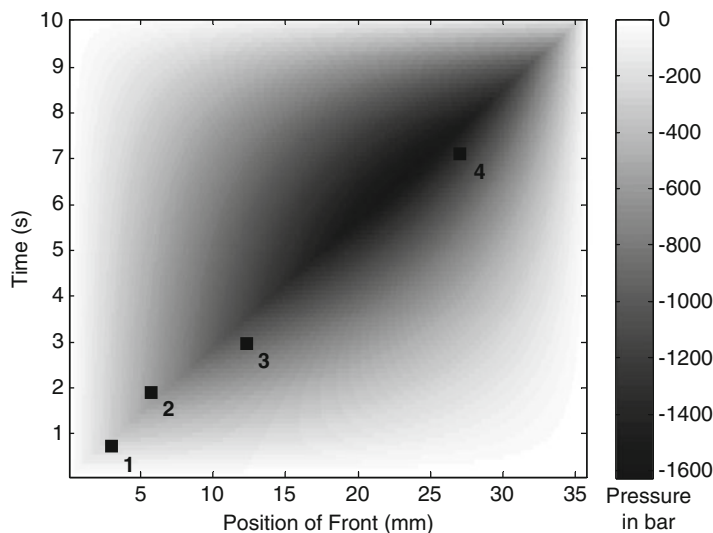
Fig. 12.6 The theoretical axial pressure in the nanochannel (*horizontal axis*) against time (*vertical axis*), generated using an experimentally determined ζ-potential of −60 mV, an applied voltage of −3 kV and solution conductivities of $K_{high} = 0.135$ S/m and $K_{low} = 0.0387$ S/m and measured channel height of 53 nm. The number next to each point represents the cycle number. The pressures at the cavitation locations were (from *left* to *right*): −280, −720, −1,050 and −1,320 bar. Due to an uncertainty in the ζ-potential of 10 % they can vary by 10 %

electrical current measurements is slightly influenced by the 50Hz-filter used and reading errors and is taken as 0.1 s.

Several subsequent four-cycle experiments were performed in three different channels at three applied voltages: −1, −2, and −3 kV, and the cavitation positions and times were recorded. In some channels cavitation always occurred at approximately the same position. In other channels the cavitation position in subsequent cycles or experiments moved to positions further down the channel, whereby a linear relationship was found between cavitation position and time. The first observation suggests there may be local fixed anomalies in the channels such as discontinuities in the ζ-potential caused by surface defects or particles. The second type of observations suggests anomalies that can be removed or displaced on cavitation, such as nanobubbles [12] or mobile particles.

Using the ζ-potential retrieved from the separate EOF measurements a prediction of the movement of the front between both solutions can be made, as well as of the spatiotemporal pressure distribution in the channel. Figure 12.6 plots these data, with superimposed the results of the cavitation experiments. In the four cycles recorded it seems that the cavitation location approximately coincides with the theoretical position of the front. This implies that the cavitation takes place at the point of lowest pressure which is the interface between the two solutions moving with the same velocity as the EOF. The lowest pressure where cavitation

occurs appears to be at data point number four, which corresponds to a pressure of $-1,320$ bar ± 10 %, based on a measured ζ-potential of -60 mV ± 10 %. The errors on the time and position also influence the exact value by a few tens of bar, though this error is much smaller. It is interesting that the last cavitation event (point number 4) seems to take place after a lower pressure was already reached elsewhere in the channel. This can be explained by assuming that cavitation still is heterogeneous, and that the first anomaly in this cycle is encountered at this position. In subsequent experiments at -3 kV on the same channel no more cavitation events were observed. This implies that the homogeneous cavitation pressure of this aqueous solution is below the lowest pressure reached in this experiment, which was calculated as $-1,630$ bar ± 10 %. Interestingly, this value is very close to the theoretical value using the thin wall approximation [3] of $-1,600$ bar for homogeneous cavitation in an observation volume of $\sim 10^{-13}$ m^3 and an observation time of ~ 1 s [3].

12.4   Conclusion

A new method for controlled liquid cavitation is described, called electrocavitation. It represents an experimentally flexible and reliable method for liquid cavitation studies and pressures below $-1,000$ bar can be easily reached. Experimental results suggest interesting data can be obtained both on cavitation at liquid impurities as on homogeneous cavitation. Indications are found that the homogeneous cavitation pressure of the aqueous solution used is below $-1,630$ bar ± 10 %.

References

1. Caupin F, Herbert E (2006) Cavitation in water: a review. Compte Rendu Phys 7:1000–1017
2. Or D, Tuller M (2002) Cavitation during desaturation of porous media under tension. Water Resour Res 38:1061
3. Rajamani S, Truskett TM, Garde S (2005) Hydrophobic hydration from small to large lengthscales: understanding and manipulating the crossover. Proc Natl Acad Sci USA 102:9475–9480
4. Herbert E, Balibar S, Caupin F (2006) Cavitation pressure in water. Phys Rev E 74:041603
5. Briggs LJ (1950) Limiting negative pressure of water. J Appl Phys 21:721–722
6. Zheng Q, Durben D, Wolf G, Angell C (1991) Liquids at large negative pressures: water at the homogeneous nucleation limit. Science 254:829–832
7. Davitt K, Rolley E, Caupin F, Arvengas A, Balibar S (2010) Water at the cavitation limit: density of the metastable liquid and size of the critical bubble. J Chem Phys 133:174507

8. Shmulovich KI, Mercury L, Thiéry R, Ramboz C, Mekki ME (2009) Experimental superheating of water and aqueous solutions. Geochim Cosmochim Acta 73:2457–2470
9. Janssen KGH, Eijkel JCT, Tas NR, de Vreede LJ, Hankemeier T, van der Linden HJ (2011) Electrocavitation in nanochannels. Proceedings MicroTAS 2011. Seattle WA, USA
10. Huang X, Gordon MJ, Zare RN (1988) Current-monitoring method for measuring the electroosmotic flow rate in capillary zone electrophoresis. Anal Chem 60:1837–1838
11. Bruus H (2007) Theoretical microfluidics. Oxford University Press, Oxford
12. Borkent B, Dammer SM, Schonherr H, Vancso GJ, Lohse D (2007) Superstability of surface nanobubbles. Phys Rev Lett 98:204502